

# Multiuser Media-based Modulation for Massive MIMO Systems

Bharath Shamasundar and A. Chockalingam

Department of ECE, Indian Institute of Science, Bangalore 560012

**Abstract**—In this paper, we consider *media-based modulation (MBM)*, an attractive modulation scheme which is getting increased research attention recently, for the uplink of a massive MIMO system. Each user is equipped with one transmit antenna with multiple radio frequency (RF) mirrors (parasitic elements) placed near it. The base station (BS) is equipped with tens to hundreds of receive antennas. MBM with  $m_{rf}$  RF mirrors and  $n_r$  receive antennas over a multipath channel has been shown to asymptotically (as  $m_{rf} \rightarrow \infty$ ) achieve the capacity of  $n_r$  parallel AWGN channels. This suggests that MBM can be attractive for use in massive MIMO systems which typically employ a large number of receive antennas at the BS. In this paper, we investigate the potential performance advantage of multiuser MBM (MU-MBM) in a massive MIMO setting. Our results show that multiuser MBM (MU-MBM) can significantly outperform other modulation schemes. For example, a bit error performance achieved using 500 receive antennas at the BS in a massive MIMO system using conventional modulation can be achieved using just 128 antennas using MU-MBM. Even multiuser spatial modulation, and generalized spatial modulation in the same massive MIMO settings require more than 200 antennas to achieve the same bit error performance. Also, recognizing that the MU-MBM signal vectors are inherently sparse, we propose an efficient MU-MBM signal detection scheme that uses compressive sensing based reconstruction algorithms like orthogonal matching pursuit (OMP), compressive sampling matching pursuit (CoSaMP), and subspace pursuit (SP).

**Keywords** – *Media-based modulation, RF mirrors, massive MIMO, compressive sensing, sparse recovery, OMP, CoSaMP, subspace pursuit.*

## I. INTRODUCTION

Media-based modulation (MBM), a promising modulation scheme for wireless communications in multipath fading environments, is attracting recent research attention [1]- [5]. The key features that make MBM different from conventional modulation are: *i*) MBM uses digitally controlled parasitic elements external to the transmit antenna that act as radio frequency (RF) mirrors to create different channel fade realizations which are used as the channel modulation alphabet, and *ii*) it uses indexing of these RF mirrors to convey additional information bits. The basic idea behind MBM can be explained as follows.

Placing RF mirrors near a transmit antenna is equivalent to placing scatterers in the propagation environment close to the transmitter. The radiation characteristics of each of these scatterers (i.e., RF mirrors) can be changed by an ON/OFF control signal applied to it. An RF mirror reflects back the incident wave originating from the transmit antenna or passes the wave depending on whether it is OFF or ON. The ON/OFF status of the mirrors is called as the mirror activation pattern (MAP). The positions of the ON mirrors and OFF mirrors change from one MAP to the other, i.e., the propagation environment close to the transmitter changes from one MAP to the other MAP. Note that in a rich scattering environment, a small perturbation

in the propagation environment will be augmented by many random reflections resulting in an independent channel. The RF mirrors create such perturbations by acting as controlled scatterers, which, in turn, create independent fade realizations for different MAPs.

If  $m_{rf}$  is the number of RF mirrors used, then  $2^{m_{rf}}$  MAPs are possible. If the transmitted signal is received through  $n_r$  receive antennas, then the collection of  $2^{m_{rf}}$   $n_r$ -length complex channel gain vectors form the MBM channel alphabet. This channel alphabet can convey  $m_{rf}$  information bits through MAP indexing. If the antenna transmits a symbol from a conventional modulation alphabet denoted by  $\mathbb{A}$ , then the spectral efficiency of MBM is  $\eta_{\text{MBM}} = m_{rf} + \log_2 |\mathbb{A}|$  bits per channel use (bpcu). An implementation of a MBM system consisting of 14 RF mirrors placed in a compact cylindrical structure with a dipole transmit antenna element placed at the center of the cylindrical structure has been reported in [3]. Early reporting of the idea of using parasitic elements for index modulation purposes (in the name ‘aerial modulation’) can be found in [6], [7].

MBM has been shown to possess attractive performance attributes, particularly when the number of receive antennas is large [1]- [5]. Specifically, MBM with  $m_{rf}$  RF mirrors and  $n_r$  receive antennas over a multipath channel has been shown to asymptotically (as  $m_{rf} \rightarrow \infty$ ) achieve the capacity of  $n_r$  parallel AWGN channels [2]. This suggests that MBM can be attractive for use in massive MIMO systems which typically employ a large number of receive antennas at the BS. However, the literature on MBM so far has focused mainly on single-user (point-to-point) communication settings. Our first contribution in this paper is that, we report MBM in multiuser massive MIMO settings and demonstrate significant performance advantages of MBM compared to conventional modulation. For example, a bit error performance achieved using 500 receive antennas at the BS in a massive MIMO system using conventional modulation can be achieved using just 128 antennas with multiuser MBM. Even multiuser spatial modulation (SM) and generalized spatial modulation (GSM) [8]- [12] in the same massive MIMO settings require more than 200 antennas to achieve the same bit error performance. This suggests that multiuser MBM can be an attractive scheme for use in the uplink of massive MIMO systems.

The second contribution relates to exploitation of the inherent sparsity in multiuser MBM signal vectors for low-complexity signal detection at the BS receiver. We resort to compressive sensing (CS) based sparse recovery algorithms for this purpose. Several efficient sparse recovery algorithms are known in the literature [13]- [21]. We propose a multiuser MBM signal detection scheme that employs greedy sparse recovery algorithms like orthogonal matching pursuit (OMP) [13], compressive sampling matching pursuit (CoSaMP) [14], and subspace pursuit (SP) [15]. Simulation results show that

the proposed detection scheme using SP achieves very good performance (e.g., significantly better performance compared to MMSE detection) at low complexity. This demonstrates that CS based sparse signal recovery approach is a natural and efficient approach for multiuser MBM signal detection in massive MIMO systems.

The rest of the paper is organized as follows. The multiuser MBM system model is introduced in Sec. II. The performance of multiuser MBM with maximum likelihood detection is presented in Sec. III. The proposed sparsity-exploiting detection scheme for multiuser MBM signal detection and its performance in massive MIMO systems are presented in Sec. IV. Conclusions are presented in Sec. V.

## II. MULTIUSER MBM SYSTEM MODEL

Consider a massive MIMO system with  $K$  uplink users and a BS with  $n_r$  receive antennas (see Fig. 1), where  $K$  is in the tens (e.g.,  $K = 16, 32$ ) and  $n_r$  is in the hundreds ( $n_r = 128, 256$ ). The users employ MBM for signal transmission. Each user has a single transmit antenna and  $m_{r,f}$  RF mirrors placed near it. In a given channel use, each user selects one of the  $2^{m_{r,f}}$  mirror activation patterns (MAPs) using  $m_{r,f}$  information bits. A mapping is done between the combinations of  $m_{r,f}$  information bits and the MAPs. An example mapping between information bits and MAPs is shown in Table I for  $m_{r,f} = 2$ . The mapping between the possible MAPs and information bits is made known a priori to both transmitter and receiver for encoding and decoding purposes, respectively.

Information bits	Mirror 1 status	Mirror 2 status
00	ON	ON
01	ON	OFF
10	OFF	ON
11	OFF	OFF

TABLE I  
MAPPING BETWEEN INFORMATION BITS AND MAPS FOR  $m_{r,f} = 2$ .

Apart from the bits conveyed through the choice of a MAP in a given channel use as described above, a symbol from a modulation alphabet  $\mathbb{A}$  (e.g., QAM, PSK) transmitted by the antenna conveys an additional  $\log_2 |\mathbb{A}|$  bits. Therefore, the spectral efficiency of a  $K$ -user MBM system is given by

$$\eta_{\text{MU-MBM}} = K(m_{r,f} + \log_2 |\mathbb{A}|) \text{ bpcu.} \quad (1)$$

For example, a multiuser MBM system with  $K = 4$ ,  $m_{r,f} = 2$ , and 4-QAM has a system spectral efficiency of 16 bpcu. An important point to note here is that the spectral efficiency per user increases linearly with the number of RF mirrors used at each user. To introduce the multiuser MBM signal set and the corresponding received signal vector at the BS, let us first formally introduce the single-user MBM signal set.

### A. Single-user MBM channel alphabet

The MBM channel alphabet of a single user is the set of all channel gain vectors corresponding to the various MAPs of that user. Let us define  $M \triangleq 2^{m_{r,f}}$ , where  $M$  is the number of possible MAPs corresponding to  $m_{r,f}$  RF mirrors. Let  $\mathbf{h}_k^m$  denote the  $n_r \times 1$  channel gain vector corresponding to the  $m$ th

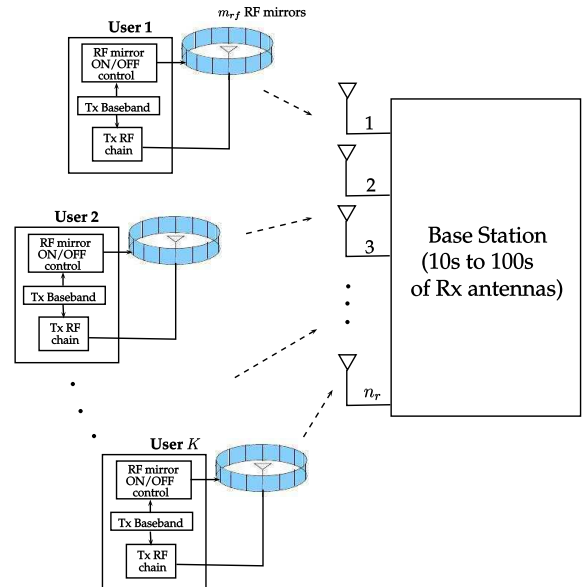


Fig. 1. Multiuser MBM in a massive MIMO system.

MAP of the  $k$ th user, where  $\mathbf{h}_k^m = [h_{1,k}^m \ h_{2,k}^m \ \dots \ h_{n_r,k}^m]^T$ ,  $h_{i,k}^m$  is the channel gain corresponding to the  $m$ th MAP of the  $k$ th user to the  $i$ th receive antenna,  $i = 1, \dots, n_r$ ,  $k = 1, \dots, K$ , and  $m = 1, \dots, M$ , and the  $h_{i,k}^m$ s are assumed to be i.i.d. and distributed as  $\mathcal{CN}(0, 1)$ . The MBM channel alphabet for the  $k$ th user, denoted by  $\mathbb{H}_k$ , is then the collection of these channel gain vectors, i.e.,  $\mathbb{H}_k = \{\mathbf{h}_k^1, \mathbf{h}_k^2, \dots, \mathbf{h}_k^M\}$ . The MBM channel alphabet of each user is estimated at the BS receiver through pilot transmission before data transmission. The number of pilot channel uses needed for the estimation of each user's channel alphabet grows exponentially in  $m_{r,f}$ . It is also noted that, while the MBM channel alphabet of each user needs to be known at the BS receiver for detection purposes, the users' transmitters need not know their channel alphabets.

### B. Single-user MBM signal set

Define  $\mathbb{A}_0 \triangleq \mathbb{A} \cup 0$ . The single-user MBM signal set, denoted by  $\mathbb{S}_{\text{SU-MBM}}$ , is the set of  $M \times 1$ -sized MBM signal vectors given by

$$\begin{aligned} \mathbb{S}_{\text{SU-MBM}} &= \{ \mathbf{s}_{m,q} \in \mathbb{A}_0^M : m = 1, \dots, M, q = 1, \dots, |\mathbb{A}| \} \\ \text{s.t. } \mathbf{s}_{m,q} &= [0, \dots, 0, \underbrace{s_q}_{m\text{th coordinate}}, 0, \dots, 0]^T, s_q \in \mathbb{A}, \end{aligned} \quad (2)$$

where  $m$  is the index of the MAP. That is, an MBM signal vector  $\mathbf{s}_{m,q}$  in (2) means a complex symbol  $s_q \in \mathbb{A}$  being transmitted on a channel with an associated channel gain vector  $\mathbf{h}^m$ , where  $\mathbf{h}^m$  is the  $n_r \times 1$  channel gain vector corresponding to the  $m$ th MAP. Therefore, the  $n_r \times 1$  received signal vector corresponding to a transmitted MBM signal vector  $\mathbf{s}_{m,q}$  can be written as

$$\mathbf{y} = s_q \mathbf{h}^m + \mathbf{n}, \quad (3)$$

where  $\mathbf{n} \in \mathbb{C}^{n_r}$  is the AWGN noise vector with  $\mathbf{n} \sim \mathcal{CN}(\mathbf{0}, \sigma^2 \mathbf{I})$ . The size of the single-user MBM signal set is  $|\mathbb{S}_{\text{SU-MBM}}| = M|\mathbb{A}|$ . For example, if  $m_{r,f} = 2$  and  $|\mathbb{A}| = 2$  (i.e., BPSK), then  $|\mathbb{S}_{\text{SU-MBM}}| = 8$ , and the corresponding MBM signal set is given by

$$\mathbb{S}_{\text{SU-MBM}} = \left\{ \begin{bmatrix} 1 \\ 0 \\ 0 \\ 0 \end{bmatrix}, \begin{bmatrix} -1 \\ 0 \\ 0 \\ 0 \end{bmatrix}, \begin{bmatrix} 0 \\ 1 \\ 0 \\ 0 \end{bmatrix}, \begin{bmatrix} 0 \\ -1 \\ 0 \\ 0 \end{bmatrix}, \begin{bmatrix} 0 \\ 0 \\ 1 \\ 0 \end{bmatrix}, \begin{bmatrix} 0 \\ 0 \\ -1 \\ 0 \end{bmatrix}, \begin{bmatrix} 0 \\ 0 \\ 0 \\ 1 \end{bmatrix}, \begin{bmatrix} 0 \\ 0 \\ 0 \\ -1 \end{bmatrix} \right\} \quad (4)$$

### C. Multiuser MBM received signal

With the above definitions of single-user MBM channel alphabet and signal set, the multiuser MBM signal set with  $K$  users is given by  $\mathbb{S}_{\text{MU-MBM}} = \mathbb{S}_{\text{SU-MBM}}^K$ . Let  $\mathbf{x}_k \in \mathbb{S}_{\text{SU-MBM}}$  denote the transmit MBM signal vector from the  $k$ th user. Let  $\mathbf{x} = [\mathbf{x}_1^T \mathbf{x}_2^T \cdots \mathbf{x}_K^T]^T \in \mathbb{S}_{\text{MU-MBM}}$  denote the vector comprising of the transmit MBM signal vectors from all the  $K$  users. Let  $\mathbf{H} \in \mathbb{C}^{n_r \times KM}$  denote the channel gain matrix given by  $\mathbf{H} = [\mathbf{H}_1 \mathbf{H}_2 \cdots \mathbf{H}_K]$ , where  $\mathbf{H}_k = [\mathbf{h}_k^1 \mathbf{h}_k^2 \cdots \mathbf{h}_k^M] \in \mathbb{C}^{n_r \times M}$ , and  $\mathbf{h}_k^m$  is the channel gain vector of the  $k$ th user corresponding to  $m$ th MAP as defined before. The  $n_r \times 1$  multiuser received signal vector at the BS is then given by

$$\mathbf{y} = \mathbf{H}\mathbf{x} + \mathbf{n}, \quad (5)$$

where  $\mathbf{n}$  is the  $n_r \times 1$  AWGN noise vector with  $\mathbf{n} \sim \mathcal{CN}(\mathbf{0}, \sigma^2 \mathbf{I})$ .

## III. PERFORMANCE OF MULTIUSER MBM

In this section, we analyze the BER performance of multiuser MBM under maximum likelihood (ML) detection. We obtain an upper bound on the BER which is tight at moderate to high SNRs. We also present a comparison between the BER performance of multiuser MBM and those of other multiuser schemes that employ conventional modulation, spatial modulation, and generalized spatial modulation.

### A. Upper bound on BER

The ML detection rule for the multiuser MBM system model in (5) is given by

$$\hat{\mathbf{x}} = \underset{\mathbf{x} \in \mathbb{S}_{\text{MU-MBM}}}{\operatorname{argmin}} \|\mathbf{y} - \mathbf{H}\mathbf{x}\|^2, \quad (6)$$

which can be written as

$$\hat{\mathbf{x}} = \underset{\mathbf{x} \in \mathbb{S}_{\text{MU-MBM}}}{\operatorname{argmin}} (\|\mathbf{H}\mathbf{x}\|^2 - 2\mathbf{y}^T \mathbf{H}\mathbf{x}). \quad (7)$$

The pairwise error probability (PEP) that the receiver decides in favor of the signal vector  $\mathbf{x}_2$  when  $\mathbf{x}_1$  was transmitted, given the channel matrix  $\mathbf{H}$  can be written as

$$\begin{aligned} PEP &= P(\mathbf{x}_1 \rightarrow \mathbf{x}_2 | \mathbf{H}) \\ &= P(2\mathbf{y}^T \mathbf{H}(\mathbf{x}_2 - \mathbf{x}_1) > (\|\mathbf{H}\mathbf{x}_2\|^2 - \|\mathbf{H}\mathbf{x}_1\|^2) | \mathbf{H}) \\ &= P(2\mathbf{n}^T \mathbf{H}(\mathbf{x}_2 - \mathbf{x}_1) > \|\mathbf{H}(\mathbf{x}_2 - \mathbf{x}_1)\|^2 | \mathbf{H}). \end{aligned} \quad (8)$$

Defining  $z \triangleq 2\mathbf{n}^T \mathbf{H}(\mathbf{x}_2 - \mathbf{x}_1)$ , we observe that  $z \sim \mathcal{N}(0, 2\sigma^2 \|\mathbf{H}(\mathbf{x}_2 - \mathbf{x}_1)\|^2)$ . Therefore, we can write

$$P(\mathbf{x}_1 \rightarrow \mathbf{x}_2 | \mathbf{H}) = Q\left(\frac{\|\mathbf{H}(\mathbf{x}_2 - \mathbf{x}_1)\|}{\sqrt{2}\sigma}\right), \quad (9)$$

where  $Q(x) = \frac{1}{\sqrt{2\pi}} \int_x^\infty e^{-\frac{t^2}{2}} dt$ . The conditional PEP expression in (9) can be written as

$$P(\mathbf{x}_1 \rightarrow \mathbf{x}_2 | \mathbf{H}) = Q\left(\sqrt{\frac{1}{2\sigma^2} \left\| \sum_{l=1}^{KM} (x_{1,l} - x_{2,l}) \mathbf{h}_l \right\|^2}\right), \quad (10)$$

where  $x_{1,l}$  and  $x_{2,l}$  are  $l$ th entries of  $\mathbf{x}_1$  and  $\mathbf{x}_2$ , respectively, and  $\mathbf{h}_l$  is the  $l$ th column of  $\mathbf{H}$ . The argument of  $Q(\cdot)$  in (10) has the central  $\chi^2$ -distribution with  $2n_r$  degrees of freedom. The computation of the unconditional PEPs requires the expectation of  $Q(\cdot)$  with respect to  $\mathbf{H}$ , which can be obtained as follows [22]:

$$\begin{aligned} P(\mathbf{x}_1 \rightarrow \mathbf{x}_2) &= \mathbb{E}_{\mathbf{H}} [P(\mathbf{x}_1 \rightarrow \mathbf{x}_2 | \mathbf{H})] \\ &= f(\alpha)^{n_r} \sum_{i=0}^{n_r-1} \binom{n_r-1+i}{i} (1-f(\alpha))^i, \end{aligned} \quad (11)$$

where  $f(\alpha) \triangleq \frac{1}{2} \left(1 - \sqrt{\frac{\alpha}{1+\alpha}}\right)$ ,  $\alpha \triangleq \frac{1}{4\sigma^2} \sum_{l=1}^{KM} \theta_l$ , and  $\theta_l \triangleq |x_{1,l} - x_{2,l}|^2$ . Now, an upper bound on the bit error probability using union bound can be obtained as

$$P_e \leq \frac{1}{2^{n_{\text{MU-MBM}}}} \sum_{\mathbf{x}_1 \in \mathbb{S}_{\text{MU-MBM}}} \sum_{\mathbf{x}_2 \in \mathbb{S}_{\text{MU-MBM}} \setminus \mathbf{x}_1} P(\mathbf{x}_1 \rightarrow \mathbf{x}_2) \frac{d_H(\mathbf{x}_1, \mathbf{x}_2)}{\eta_{\text{MU-MBM}}}, \quad (12)$$

where  $d_H(\mathbf{x}_1, \mathbf{x}_2)$  is the Hamming distance between the bit mappings corresponding to  $\mathbf{x}_1$  and  $\mathbf{x}_2$ .

### B. Numerical results

We evaluated the BER performance of multiuser MBM (MU-MBM) using the BER upper bound derived above as well as simulations. For the purpose of initial comparisons with other systems, we consider a MU-MBM system with  $K = 2$ ,  $n_r = 8$ ,  $m_{r,f} = 3$ , BPSK, and 4 bpcu per user. Let  $n_t$  and  $n_{r,f}$  denote the number transmit antennas and transmit RF chains, respectively, at each user. Note that in the considered MU-MBM system, each user uses one transmit antenna and one transmit RF chain, i.e.,  $n_t = n_{r,f} = 1$ . We compare the performance of the above MU-MBM system with those of three other multiuser systems which use *i*) conventional modulation (CM), *ii*) spatial modulation (SM), and *iii*) generalized spatial modulation (GSM). The multiuser system with conventional modulation (MU-CM) uses  $n_t = n_{r,f} = 1$  at each user and employs 16-QAM to achieve the same spectral efficiency of 4 bpcu per user. The multiuser system with SM (MU-SM) uses  $n_t = 2$ ,  $n_{r,f} = 1$ , and 8-QAM, achieving a spectral efficiency of  $\log_2 n_t + \log_2 |\mathbb{A}| = \log_2 2 + \log_2 8 = 4$  bpcu per user. The multiuser system with GSM (MU-GSM) uses  $n_t = 4$ ,  $n_{r,f} = 2$ , and BPSK, achieving a spectral efficiency of  $\lfloor \log_2 \binom{n_t}{n_{r,f}} \rfloor + \log_2 |\mathbb{A}| = \lfloor \log_2 \binom{4}{2} \rfloor + \log_2 2 = 4$  bpcu per user.

Figure 2 shows the BER performance of the MU-MBM, MU-CM, MU-SM, and MU-GSM systems described above. First, it can be observed that the analytical upper bound is very tight at moderate to high SNRs. Next, in terms of performance comparison between the considered systems, the following inferences can be drawn from Fig. 2.

- The MU-MBM system achieves the best performance among all the four systems considered. For example, MU-MBM performs better by about 5 dB, 4 dB, 2.5 dB compared to MU-CM, MU-SM, and MU-GSM systems, respectively, at a BER of  $10^{-5}$ .
- The better performance of MU-MBM can be attributed to more bits being conveyed through mirror indexing, which allows MU-MBM to use lower-order modulation



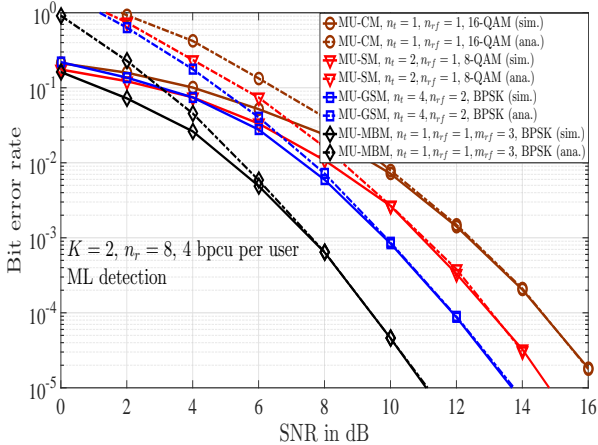


Fig. 2. BER performance of MU-MBM, MU-CM, MU-SM, and MU-GSM with  $K = 2$ ,  $n_r = 8$ , 4 bpcu per user, and ML detection. Analysis and simulations.

alphabets (BPSK) compared to other systems which may need higher-order alphabets (8-QAM, 16-QAM) to achieve the same spectral efficiency.

- MU-MBM performs better than MU-GSM though both use BPSK in this example. This can be attributed to the good distance properties of the MBM signal set [2].

Note that though the results in Fig. 2 illustrate the performance superiority of MU-MBM over MU-CM, MU-SM, and MU-GSM, they are presented only for a small system with  $K = 2$  and  $n_r = 8$ . This is because ML detection is prohibitively complex for systems with large  $K$  and  $n_r$  (ML detection is exponentially complex in  $K$ ). However, massive MIMO systems are characterized by  $K$  in the tens and  $n_r$  in the hundreds. Therefore, low-complexity detection schemes which scale well for such large-scale MU-MBM systems are needed. To address this need, we resort to exploiting the inherent sparse nature of the MBM signal vectors, and devise a compressive sensing based detection algorithm in the following section.

#### IV. SPARSITY-EXPLOITING DETECTION OF MULTIUSER MBM SIGNALS

It is evident from the example signal set in (4) that the MBM signal vectors are inherently sparse. An MBM signal vector has only one non-zero element out of  $M$  elements, leading to a sparsity factor of  $1/M$ . For example, consider an MBM signal set with  $m_{r,f} = 4$  and  $M = 2^{m_{r,f}} = 16$ . Out of 16 elements in a signal vector, only one element is non-zero resulting in a sparsity factor of  $1/16$ . Exploitation of this inherent sparsity to devise detection algorithms can lead to efficient signal detection at low complexities. Accordingly, we propose a low-complexity MU-MBM signal detection scheme that employs compressive sensing based sparse reconstruction algorithms like OMP, CoSaMP, and SP.

##### A. Proposed sparsity-exploiting detection algorithm

We first model the MU-MBM signal detection problem as a sparse reconstruction problem and then employ greedy algorithms for signal detection. Sparse reconstruction is concerned with finding an approximate solution to the following problem

[23]:

$$\min_{\mathbf{x}} \|\mathbf{x}\|_0 \text{ subject to } \mathbf{y} = \Phi \mathbf{x} + \mathbf{n}, \quad (13)$$

where  $\Phi \in \mathbb{C}^{m \times n}$  is called the measurement matrix,  $\mathbf{x} \in \mathbb{C}^n$  is the complex input signal vector,  $\mathbf{y} \in \mathbb{C}^m$  is the noisy observation corresponding to the input signal, and  $\mathbf{n} \in \mathbb{C}^m$  is the complex noise vector. The MU-MBM signal detection problem at the BS in (5) can be modeled as a sparse recovery problem in (13), with the measurement matrix being the channel matrix  $\mathbf{H} \in \mathbb{C}^{n_r \times K M}$ , the noisy observation being the received signal vector  $\mathbf{y} \in \mathbb{C}^{n_r}$ , and the input being the MU-MBM transmit signal vector  $\mathbf{x} \in \mathbb{S}_{\text{MU-MBM}}$ . The noise vector is additive complex Gaussian with  $\mathbf{n} \sim \mathcal{CN}(\mathbf{0}, \sigma^2 \mathbf{I})$ .

Greedy algorithms achieve sparse reconstruction in an iterative manner. They decompose the problem of sparse recovery into a two step process; recover the support of the sparse vector first, and then obtain the non-zero values over this support. For example, OMP starts with an initial empty support set, an initial solution  $\mathbf{x}^0 = \mathbf{0}$ , and an initial residue  $\mathbf{r}^0 = \mathbf{y} - \mathbf{H}\mathbf{x}^0 = \mathbf{y}$ . In each step, OMP updates one coordinate of the vector  $\mathbf{x}$  based on the correlation values between the residue vector and the columns of the  $\mathbf{H}$  matrix. In the  $k$ th iteration, an element  $j_0$  given by

$$j_0 = \operatorname{argmax}_{j \notin \mathcal{S}^{k-1}} \frac{\mathbf{h}_j^T \mathbf{r}^{k-1}}{\|\mathbf{h}_j\|_2}$$

is added to the support set, where  $\mathbf{h}_j$  is the  $j$ th column of  $\mathbf{H}$ , and  $\mathcal{S}^{k-1}$  and  $\mathbf{r}^{k-1}$  are the support set and residue after  $k-1$  iterations, respectively. The entries of  $\mathbf{x}$  corresponding to the obtained support set are computed using least squares. This process is iterated till the stopping criteria is met. The stopping criteria can be either a specified error threshold or a specified level of sparsity.

In the SP algorithm, instead of updating one coordinate of  $\mathbf{x}$  at a time as in OMP,  $K$  coordinates are updated at once. The major difference between OMP and SP is the following. In OMP, the support set is generated sequentially. It starts with an empty set and adds one element in every iteration to the existing support set. An element added to the support set can not be removed until the algorithm terminates. In contrast, SP provides flexibility of refining the support set in every iteration. CoSaMP is similar to SP except that it updates  $2K$  coordinates in each iteration to the support set instead of updating  $K$  coordinates as in SP. CoSaMP and SP have superior reconstruction capability comparable to convex relaxation methods [14], [15]. **Algorithm 1** shows the listing of the pseudo-code of the proposed sparsity-exploiting detection algorithm for MU-MBM signals.

SR in **Algorithm 1** denotes the sparse recovery algorithm, which can be any one of OMP, CoSaMP, and SP. The signal vector reconstructed by the sparse recovery algorithm is denoted by  $\hat{\mathbf{x}}_r$ . Detecting the MU-MBM signal vector involves detecting the MBM signal vector transmitted by each user. An MBM signal vector from a user has exactly one non-zero entry out of  $M$  entries as observed in the example MBM signal set in (4). Hence, SR is expected to reconstruct a MU-MBM signal vector such that the MBM signal sub-vector corresponding to a given user has only one non-zero entry. But this constraint on the expected support set is not built in

---

**Algorithm 1** Proposed sparsity-exploiting algorithm for MU-MBM signal detection

---

```

1: Inputs:  $\mathbf{y}, \mathbf{H}, K$ 
2: Initialize:  $j = 0$ 
3: repeat
4:    $\hat{\mathbf{x}}_r = \text{SR}(\mathbf{y}, \mathbf{H}, K + j) \triangleright$  Sparse Recovery algorithm
5:    $\mathbf{u}^j = \text{UAP}(\hat{\mathbf{x}}_r) \triangleright$  Extract User Activity Pattern
6:   if  $\|\mathbf{u}^j\|_0 = K$ 
7:     for  $k = 1$  to  $K$ 
8:        $\hat{\mathbf{x}}^k = \underset{\mathbf{s} \in \mathbb{S}_{\text{SU-MBM}}}{\text{argmin}} \|\hat{\mathbf{x}}_r^k - \mathbf{s}\|^2 \triangleright$  Nearest MBM signal mapping
9:     end for
10:    break;
11:   else  $j = j + 1$ 
12:   end if
13: until  $j < K(M - 1)$ 
14: Output: The estimated MU-MBM signal vector

```

$$\hat{\mathbf{x}} = [\hat{\mathbf{x}}^1, \hat{\mathbf{x}}^2, \dots, \hat{\mathbf{x}}^K]^T$$


---

the general sparse recovery algorithms. In general, a sparse recovery algorithm can output  $K$  non-zero elements at any of the  $KM$  locations of  $\hat{\mathbf{x}}_r$ . To overcome this issue, we define user activity pattern (UAP), denoted by  $\mathbf{u}$ , as a  $K$ -length vector with  $k$ th entry as  $\mathbf{u}_k = 1$  if there is at least one non-zero entry in the  $k$ th user's recovered MBM signal vector, and  $\mathbf{u}_k = 0$  otherwise. A valid reconstructed signal vector is one which has all ones in  $\mathbf{u}$ . SR is used multiple times with a range of sparsity estimates starting from  $K$  ( $K + j$  in the algorithm listing) till the valid UAP is obtained (i.e., till the algorithm reconstructs at least one non-zero entry for each user's MBM signal vector).

In the algorithm listing,  $\mathbf{u}^j$  denotes the UAP at the  $j$ th iteration. On recovering an  $\hat{\mathbf{x}}_r$  with valid UAP, the MBM signal vector of each user is mapped to the nearest (in the Euclidean sense) MBM signal vector in  $\mathbb{S}_{\text{SU-MBM}}$ . This is shown in the Step 8 in the algorithm listing, where  $\hat{\mathbf{x}}_r^k$  denotes the recovered MBM signal vector of the  $k$ th user and  $\hat{\mathbf{x}}^k$  denotes the MBM signal vector to which  $\hat{\mathbf{x}}_r^k$  gets mapped to. Finally, the MU-MBM signal vector is obtained by concatenating the detected MBM signal vectors of all the users, i.e.,  $\hat{\mathbf{x}} = [\hat{\mathbf{x}}^1, \hat{\mathbf{x}}^2, \dots, \hat{\mathbf{x}}^K]^T$ .

The decoding of information bits from the detected MBM signal vector of a given user involves decoding of mirror index bits and QAM symbol bits of that user. The mirror index bits are decoded from the MAP of the detected MBM signal vector and the QAM bits are decoded from the detected QAM symbol.

### B. Performance results in massive MIMO system

In this subsection, we present the BER performance of MU-MBM systems in a massive MIMO setting (i.e.,  $K$  in the tens and  $n_r$  in the hundreds) when the proposed **Algorithm 1** is used for MU-MBM signal detection at the BS. In the same massive MIMO setting, we evaluate the performance of other systems that use conventional modulation (MU-CM), spatial modulation (MU-SM), and generalized spatial modulation (MU-GSM), and compare them with the perfor-

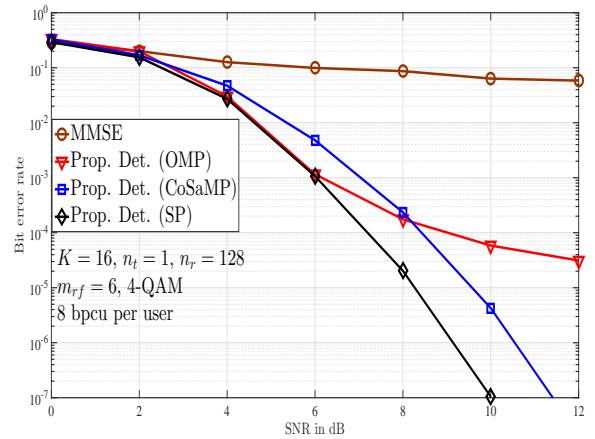


Fig. 3. BER performance of MU-MBM in a massive MIMO system with  $K = 16$ ,  $n_r = 128$ ,  $n_t = 1$ ,  $n_{r,f} = 1$ ,  $m_{r,f} = 6$ , 4-QAM, 8 bpcu per user, using the proposed detection algorithm. MMSE detection performance is also shown for comparison.

mance achieved by MU-MBM. The proposed **Algorithm 1** is also used for the detection of MU-SM and MU-GSM. It is noted that the MU-SM and MU-GSM signal vectors are also sparse to some extent; the sparsity factors in MU-SM and MU-GSM are  $1/n_t$  and  $n_{r,f}/n_t$ , respectively. So the use of the proposed algorithm for detection of these signals is also appropriate. ML detection is used to detect MU-CM signals (this is possible for MU-CM with sphere decoding for  $K = 16$ , i.e., 32 real dimensions).

*MU-MBM performance using proposed algorithm:* Figure 3 shows the performance of MU-MBM system using the proposed algorithm with *i*) OMP, *ii*) CoSaMP, and *iii*) SP. MMSE detection performance is also shown for comparison. A massive MIMO system with  $K = 16$  and  $n_r = 128$  is considered. Each user uses  $n_t = 1$ ,  $n_{r,f} = 1$ ,  $m_{r,f} = 6$ , and 4-QAM. This results in a spectral efficiency of 8 bpcu per user, and a sparsity factor of  $1/64$ . From Fig. 3, we observe that the proposed algorithm with OMP, CoSaMP, and SP achieve significantly better performance compared to MMSE. Among the the use of OMP, CoSaMP, and SP in the proposed algorithm, use of SP gives the best performance. This illustrates the superior reconstruction/detection advantage of the proposed algorithm with SP. We will use the proposed algorithm with SP in the subsequent performance results figures. It is noted that the complexity of proposed algorithm is also quite favorable; the complexity of the proposed algorithm with SP and that of MMSE are  $O(K^2 M n_r)$  and  $O(K^3 M^3)$ , respectively.

*Performance of MU-MBM, MU-SM, MU-GSM:* Figure 4 shows a BER performance comparison between MU-MBM, MU-CM, MU-SM, and MU-GSM in a massive MIMO setting with  $K = 16$  and  $n_r = 128$ . The proposed algorithm with SP is used for detection in MU-MBM, MU-SM, and MU-GSM. ML detection is used for MU-CM. The spectral efficiency is fixed at 5 bpcu per user for all the four schemes. MU-MBM achieves this spectral efficiency with  $n_t = 1$ ,  $n_{r,f} = 1$ ,  $m_{r,f} = 3$ , and 4-QAM. MU-CM uses  $n_t = 1$ ,  $n_{r,f} = 1$ , and 32-QAM to achieve 5 bpcu per user. To achieve the same 5 bpcu per user, MU-SM uses  $n_t = 4$ ,  $n_{r,f} = 1$ , and 8-QAM, and MU-GSM uses  $n_t = 5$ ,  $n_{r,f} = 2$ , and BPSK. The sparsity factors in MU-MBM, MU-SM, and MU-GSM

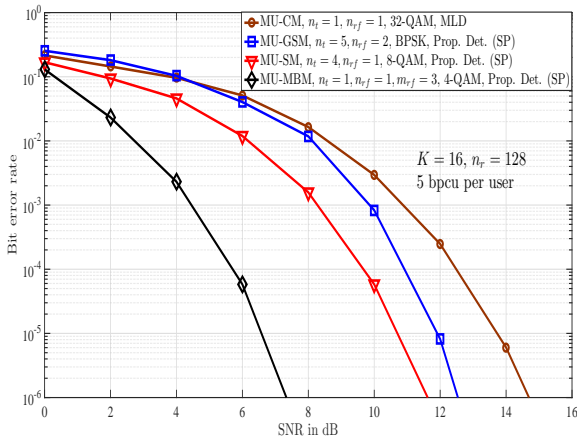


Fig. 4. BER performance MU-MBM, MU-CM, MU-SM, and MU-GSM in a massive MIMO setting with  $K = 16$ ,  $n_r = 128$ , and 5 bpcu per user.

are  $1/8$ ,  $1/4$ , and  $2/5$ , respectively. It can be seen that, MU-MBM clearly outperforms MU-CM, MU-SM, and MU-GSM. For example, at a BER of  $10^{-5}$ , MU-MBM outperforms MU-CM, MU-GSM, and MU-SM by about 7 dB, 5 dB, and 4 dB, respectively. The performance advantage of MU-MBM can be mainly attributed to its better signal distance properties [2]. MU-MBM is also benefited by its lower sparsity factor as well as the possibility of using lower-order QAM size because of additional bits being conveyed through indexing mirrors.

*Effect of number of BS receive antennas:* Figure 5 shows an interesting result which demonstrates MU-MBM's increasing performance gain compared to MU-CM, MU-SM, and MU-GSM as the number of BS receive antennas is increased. A massive MIMO system with  $K = 16$  and 5 bpcu per user is considered. The parameters of the four schemes are the same as those in Fig. 4 except that here SNR is fixed at 4 dB and  $n_r$  is varied from 48 to 624. It is interesting to observe that a performance that could be achieved using 500 antennas at the BS in a massive MIMO system that uses conventional modulation ( $3 \times 10^{-3}$  BER for MU-CM at  $n_r = 500$  with ML detection) can be achieved using just 128 antennas when MU-MBM is used ( $3 \times 10^{-3}$  BER for MU-MBM at  $n_r = 128$  with proposed detection). MU-SM and MU-GSM also achieve better performance compared to MU-CM, but they too require more than 200 antennas to achieve the same BER. This increasing performance advantage of MU-MBM for increasing  $n_r$  can be mainly attributed to its better signal distance properties particularly when  $n_r$  is large [2]. This indicates that multiuser MBM can be a very good scheme for use in the uplink of massive MIMO systems.

## V. CONCLUSIONS

We investigated the use of media-based modulation (MBM), a recent and attractive modulation scheme that employs RF mirrors (parasitic elements) to convey additional information bits through indexing of these mirrors, in massive MIMO systems. Our results demonstrated significant performance advantages possible in multiuser MBM compared to multiuser schemes that employ conventional modulation, spatial modulation, and generalized spatial modulation. Motivated by the possibility of exploiting the inherent sparsity in multiuser MBM signal vectors, we proposed a detection scheme

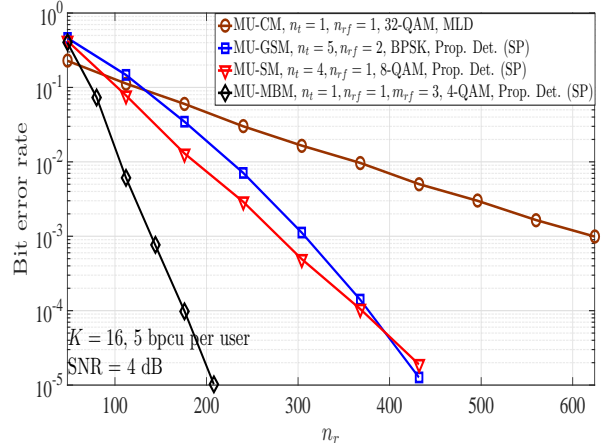


Fig. 5. BER performance MU-MBM, MU-CM, MU-SM, and MU-GSM as a function of  $n_r$  in a massive MIMO setting with  $K = 16$ , 5 bpcu per user, and SNR = 4 dB.

based on compressive sensing algorithms like OMP, CoSaMP, and subspace pursuit. The proposed detection scheme was shown to achieve very good performance (e.g., significantly better performance compared to MMSE detection) at low complexity, making it suited for multiuser MBM signal detection in massive MIMO systems. Channel estimation, effect of imperfect knowledge of the channel alphabet at the receiver, and effect of spatial correlation are interesting topics for further investigation.

## REFERENCES

- [1] A. K. Khandani, "Media-based modulation: a new approach to wireless transmission," *Proc. IEEE ISIT'2013*, pp. 3050-3054, Jul. 2013.
- [2] A. K. Khandani, "Media-based modulation: converting static Rayleigh fading to AWGN," *Proc. IEEE ISIT'2014*, pp. 1549-1553, Jun.-Jul. 2014.
- [3] E. Seifi, M. Atamanesh, and A. K. Khandani, "Media-based modulation: a new frontier in wireless communications," online arXiv:1507.07516v3 [cs.IT] 7 Oct. 2015.
- [4] Y. Naresh and A. Chockalingam, "On media-based modulation using RF mirrors," *Proc. ITA'2016*, Feb. 2016. Online arXiv:1601.06978v2 [cs.IT] 22 Oct 2016. Accepted in *IEEE Trans. Veh. Tech.*
- [5] E. Seifi, M. Atamanesh, A. K. Khandani, "Media-based MIMO: outperforming known limits in wireless," *Proc. IEEE ICC'2016*, pp. 1-7, May 2016.
- [6] O. N. Alrabadi, A. Kalis, C. B. Papadias, R. Prasad, "Aerial modulation for high order PSK transmission schemes," *Proc. Wireless VITAE 2009*, pp. 823-826, May 2009.
- [7] O. N. Alrabadi, A. Kalis, C. B. Papadias, and R. Prasad, "A universal encoding scheme for MIMO transmission using a single active element for PSK modulation schemes," *IEEE Trans. Wireless Commun.*, vol. 8, no. 10, pp. 5133-5142, Oct. 2009.
- [8] M. Di Renzo, H. Haas, A. Ghayeb, S. Sugiura, and L. Hanzo, "Spatial modulation for generalized MIMO: challenges, opportunities and implementation," *Proc. of the IEEE*, vol. 102, no. 1, pp. 56-103, Jan. 2014.
- [9] A. Chockalingam and B. S. Rajan, *Large MIMO Systems*, Cambridge Univ. Press, Feb. 2014.
- [10] J. Wang, S. Jia, and J. Song, "Generalised spatial modulation system with multiple active transmit antennas and low complexity detection scheme," *IEEE Trans. Wireless Commun.*, vol. 11, no. 4, pp. 1605-1615, Apr. 2012.
- [11] T. Datta and A. Chockalingam, "On generalized spatial modulation," *Proc. IEEE WCNC'2013*, pp. 2716-2721, Apr. 2013.
- [12] T. L. Narasimhan, P. Raviteja, and A. Chockalingam, "Generalized spatial modulation in large-scale multiuser MIMO systems," *IEEE Trans. Wireless Commun.*, vol. 14, no. 7, pp. 3764-3779, Jul. 2015.
- [13] J. A. Tropp and A. C. Gilbert, "Signal recovery from random measurements via orthogonal matching pursuit," *IEEE Trans. Inform. Theory*, vol. 53, no. 12, pp. 4655-4666, Dec. 2007.
- [14] D. Needell and J. A. Tropp, "CoSaMP: iterative signal recovery from incomplete and inaccurate samples," *Applied and Computational Harmonic Analysis* 26.3 (2009): 301-321.

- [15] W. Dai and O. Milenkovic, "Subspace pursuit for compressive sensing signal reconstruction," *IEEE Trans. Inform. Theory*, vol. 55, no. 5, pp. 2230-2249, May 2009.
- [16] N. B. Karahanoglu, and H. Erdogan, "A\* orthogonal matching pursuit: best-first search for compressed sensing signal recovery," *Digital Signal Processing*, 22(4), pp. 555-568, 2012.
- [17] D. Donoho, Y. Tsaig, I. Drori, and J.-L. Starck, "Sparse solution of underdetermined systems of linear equations by stagewise orthogonal matching pursuit," *IEEE Trans. Inform. Theory*, vol. 58, no. 2, pp. 1094-1121, Feb. 2012.
- [18] S. S. Chen, D. L. Donoho, and M. A. Saunders, "Atomic decomposition by basis pursuit," *SIAM review*, 43(1), pp. 129-159, 2001.
- [19] B. Efron, T. Hastie, I. Johnstone, and R. Tibshirani, "Least angle regression," *Annals of statistics*, vol. 32, no. 2, pp. 407-451, 2004.
- [20] R. Tibshirani, "Regression shrinkage and selection via the lasso," *J. Royal Statistical Society. Series B (Methodological)*, vol. 8, no. 1, pp. 267-288, 1996.
- [21] D. Needell and R. Vershynin, "Uniform uncertainty principle and signal recovery via regularized orthogonal matching pursuit," *Foundations of computational mathematics*, 9(3), pp. 317-334, 2009.
- [22] M. S. Alouini and G. Goldsmith, "A unified approach for calculating error rates of linearly modulated signals over generalized fading channels," *IEEE Trans. Commun.*, vol. 47, no. 9, pp. 1324-1334, Sep. 1999.
- [23] M. Elad, *Sparse and Redundant Representations: From Theory to Applications in Signal Processing*, Springer New York, 2010.